ELSEVIER

Journal of Nuclear Materials 264 (1999) 228–233

journal of nuclear materials

Quantitative determination of the bulk deuterium content of zirconium alloys using nuclear reaction analysis

Z. Qin *, W.N. Lennard, C-S. Zhang, K. Griffiths, P.R. Norton

Interface Science Western, University of Western Ontario, London Ont., Canada N6A 3K7

Received 5 May 1998; accepted 11 June 1998

Abstract

The use of the D(^{3}He,p)^{4}He reaction to study the bulk deuterium concentration in thick Zr alloy targets has been reported previously. In the present paper, we report on new measurements where the technique is extended to larger sample depths using higher projectile energies. This development is important since deuterium is known to concentrate at free surfaces and defects that may occur near surfaces; this effect might yield values unrepresentatively higher than the true bulk concentration. The bulk concentration has been extracted from a detailed comparison of experimental data with simulated proton spectra. In contrast to conclusions reached in an earlier study, the effect of ion beam desorption is unimportant with regard to the measurement of bulk deuterium concentrations when modest ^{3}He fluences are used. Analyses using beams at energies of 2 and 4.5 MeV are consistent and in good agreement with bulk deuterium concentration measured by high vacuum extraction mass spectrometry (HVEMS).

PACS: 81.70.-q

1. Introduction

Studies of the behaviour of deuterium in zirconium alloys have attracted a lot of attention [1], because the deuterium in the material plays an important role in determining the lifetime of nuclear reactor components made from Zr alloys such as Zr–2.5% Nb. If deuterium pickup during reactor operation exceeds the terminal solid solubility (TSS), failure of the components can occur due to delayed hydride cracking (DHC) and the formation of hydride blisters.

High vacuum extraction mass spectroscopy (HVEMS) is the most reliable technique currently in use for measuring the deuterium and hydrogen content of alloys [2]. The sample is degassed in a calibrated volume at an elevated temperature, from ~1000°C up to near the melting point. If the chamber is designed according to UHV technology and the initial pressure is $<10^{-6}$ Pa, the entire pressure increase can be attributed to the release of dissolved gases. The evolved gases are analysed by mass spectroscopy for the H/D ratio. However, since HVEMS is inherently a destructive technique, it is unsuitable for routine analyses, e.g., to monitor the changes of D concentration during a process designed to remove deuterium non-destructively.

Nuclear reaction analysis (NRA) is generally a non-destructive ion beam technique used to determine the elemental composition, and in some cases the depth profiles, of light elements in bulk materials from the first few hundred Ångstroms up to a few micrometers depth in the sample. For reviews on NRA and other ion beam techniques, the reader is directed to the Ion Beam Handbook [3].

Previous studies [4,5] have described applications of the NRA technique for extracting D depth distributions. Attention has focussed on the near-surface region, where significant concentration enhancements are always observed. In the present work, the goal was to make contact between the HVEMS and NRA techniques for bulk assay of CANDU pressure tubes (Zr–

* Corresponding author. Tel.: 1-519 679 2111(ext. 6326); fax: 1-519 661 3022; e-mail: zqin@julian.uwo.ca.

0022-3115/99/$ – see front matter
PII: S0022-3115(98)00465-6

2.5% Nb alloy). Although ion beam desorption effects can be observed, we will show that such effects are unimportant when modest ^{3}He fluences are used.

2. NRA energy spectrum method

The NRA technique involves measurements of the energy and flux of radiation (charged particles, γ-rays) resulting from nuclear interactions of the incident ions with atoms of the target material. Thus, NRA is isotope-specific and is often applied to light target nuclei which exhibit resonant nuclear reactions. An example is the reaction D(^{3}He,p)^{4}He which shows a broad resonance around 0.63 MeV [6].

A typical setup for an NRA experiment is shown schematically in Fig. 1. An incident monoenergetic ion beam of energy E_0 impinges on a target which is tilted to an angle θ_i . Charged particle reaction products having energy E_p are emitted from the target and detected by a silicon charged particle detector positioned at an angle θ_d and at a distance R_d. A filter of Al foil or Mylar (poly(ethylene terephthalate)) is positioned in front of the detector to stop the intense flux of elastically scattered particles.

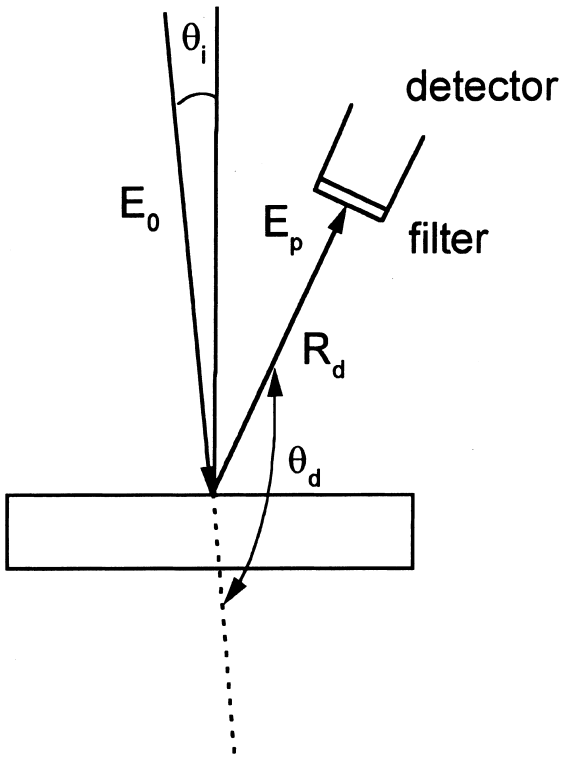

Fig. 1. Schematic diagram of the NRA experimental setup.

For the D(^{3}He,p)^{4}He reaction, the emitted proton energy increases (at backward angles, $\theta_d > 100°$) as the ^{3}He energy decreases. Since the incident ions lose energy when penetrating into the target, the emitted protons emanating from some depth have higher energies than those emitted from near the target surface. Depth information for the deuterium can be derived from a measurement of the proton energy distribution. Due to the large energy release (Q-value $\sim$18 MeV for the D(^{3}He,p)^{4}He reaction), the emitted protons have energies in the range 12–14 MeV. To analyse a full energy spectrum, the depletion (or sensitive) depth of the detector must be greater than the projected range of the energetic protons in silicon (i.e. $\sim$1.3 mm). It is conventional to relate the incident ^{3}He ion energy to the 'probing depth' in a sample. To this end, we define the probing depth to be that depth for which the cross section has decreased to a value of 10% of its maximum value. Thus, in using beams of 2 and 4.5 MeV ^{3}He, the corresponding probing depths in the pressure tube samples are $\sim$4 and $\sim$13 μm, respectively, for normal incidence, $\theta_i = 0$. It is worth noting that for higher ^{3}He energies, there are large deviations from an isotropic angular distribution of emitted particles [7].

The procedure for simulating proton energy spectra has been described in detail [5,8]. Briefly, the sample under analysis is divided into thin layers (we choose a layer thickness corresponding to 0.1% of the energy loss of the incident beam in the first layer), and the detector is divided into a grid. The energy spectrum $F(E,E_0)$ is then calculated from a summation over all layers j and all elements i of the grid,

$$F(E,E_0) = \sum_{i,j} \frac{\Delta Y_{ij}(E_0)}{\sqrt{2\pi} W_{ij}(E)} \exp\left[-\frac{(E-E_{ij})^2}{2W_{ij}^2(E)}\right], \qquad (1)$$

where ΔY_{ij} and E_{ij} are the yield and average energy, respectively, detected at the ith element of the detector grid, of the protons which are originally generated at the jth layer of the target, and W_{ij} is the variance arising from all contributions such as energy loss straggling and detector resolution. This procedure takes into account the kinematic broadening arising from the finite detector size, as well as the energy loss and energy loss straggling along both the inward (^{3}He) and outward (^{1}H) paths.

In order to calibrate the dispersion of the pulse height spectrum, an Au target implanted with 35 keV ^{3}He ions to a fluence of 1.71×10^{21} m^{-2} was bombarded by deuterons of energy 0.5 MeV. The inverse nuclear reaction ^{3}He(D,p)^{4}He also produces high energy protons whose energy distribution can be calculated from a knowledge of the range and range straggling of ^{3}He in Au. We have taken experimentally measured values of 98.9 and 49.2 nm, respectively [9], for these parameters. In this work, small deviations from pulse height linearity as described in Ref. [10] can be safely ignored.

The detector pulse height is obtained after accounting for the energy loss on both the inward path (for deuterons) and the outward path (for protons): specifically, the 500 keV incident D beam reaches an average energy of 477.8 keV in penetrating to an average depth of 98.9 nm in the Au target. The protons are emitted at that depth with an initial average energy of 13.599 MeV, slowing to 13.596 MeV in escaping from the target and

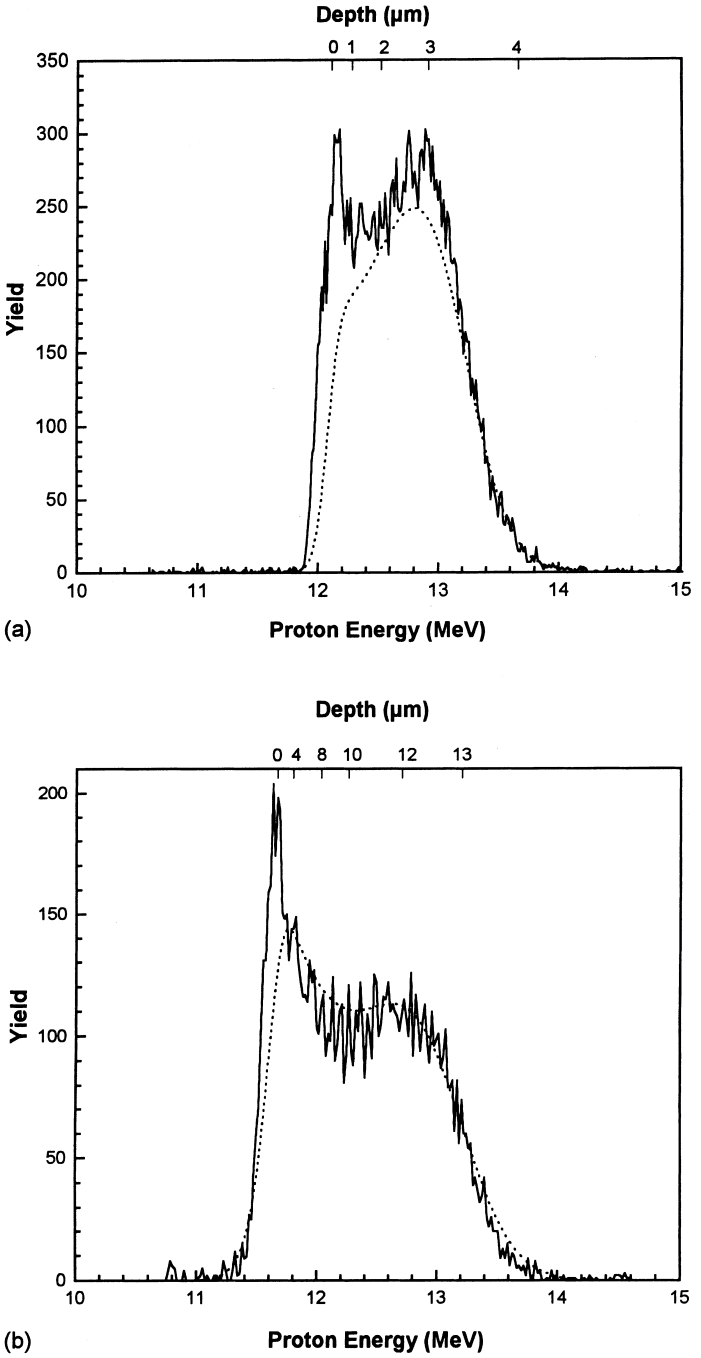

Fig. 2. Experimentally measured and simulated (shown by dotted curves) proton energy spectra for: (a) 2 MeV; (b) 4.5 MeV ^{3}He ions. The simulations have been performed assuming a constant (bulk) concentration of 117 ppmw. The depth scale as determined from the measured proton energy is shown on the top axes.

are detected at an average energy of 13.541 MeV after traversing a 12 μm Mylar film. The energy loss effect of this absorber foil is thus easily taken into account.

3. Results and discussion

NRA is performed at Interface Science Western at the University of Western Ontario using energetic ^{3}He ion beams from the 2.5 MV van de Graaff and the 1.7 MV high current Tandetron accelerators. For the van de Graaff (2 MeV) measurements the detector, which has a depletion depth of 2 mm and which was covered by a 12 μm Mylar and a ∅6.5 mm aperture, was located at $\theta_d = 150°$ and $R_d = 41.5$ mm. For the Tandetron (4.5 MeV) measurements the detector, which has a depletion depth of 1.5 mm and which was covered by a 36 μm Mylar and a ∅6.35 mm aperture, was located at $\theta_d = 138°$ and $R_d = 65.8$ mm. The target tilt angle, θ_i, was always 0°.

The samples used were offcuts from CANDU pressure tubes (Zr–2.5% Nb alloy). They were subjected to 1% D_2O in ultrahigh purity argon at a flow rate 167 mm^3 s^{-1} (STP) for 4 days at 300°C followed by thermal annealing in ultrahigh purity argon at the same flow rate and the same temperature for 16 days. The samples were then cut into pieces each of the size of $4.6 \times 4.2 \times 9.8$ mm^3 by a low speed diamond saw. The bulk concentration of deuterium is 117 ppmw (for D in Zr, 1 ppmw = 45.61 ppma = 1.935×10^{24} D atoms m^{-3}) as measured by HVEMS at AECL.

Typical measured energy spectra are shown in Fig. 2 corresponding to the 2 MeV $^3He^+$ beam at a particle current of ~100 nA for a fluence of 40 μC (Fig. 2(a)) and the 4.5 MeV $^3He^{++}$ beam at a particle current of ~15 nA for a fluence of 50 μC (Fig. 2(b)). The actual measured beam spot sizes were $\sim 2 \times 2$ mm^2 for the 2 MeV measurements and $\sim 1 \times 1$ mm^2 for the 4.5 MeV measurements. Fig. 2 also shows the results for spectra simulated for the same experimental conditions and assuming a uniform distribution of D in the sample with a concentration of 117 ppmw. The upper abscissa scale shows the appropriate depth scales, determined from the nuclear reaction kinematics and using accepted stopping powers [11] for both the ^{3}He and ^{1}H ions.

The D depth distribution is obtained by taking the ratio between the proton pulse height spectrum and the simulation in a point-by-point manner. Results are shown in Fig. 3. The uncertainties are estimated from the statistical uncertainty in the yield, together with estimates arising from uncertainties in the cross section, detector angle, etc. It is apparent that a strong near-surface enhancement of D exists up to a depth of ~1.3 μm. Beyond the surface-enhanced region, both curves become constant and are in good absolute agreement with each other. The plateaus, corresponding to the concentration of the bulk, are consistent with the average deuterium concentration obtained by HVEMS.

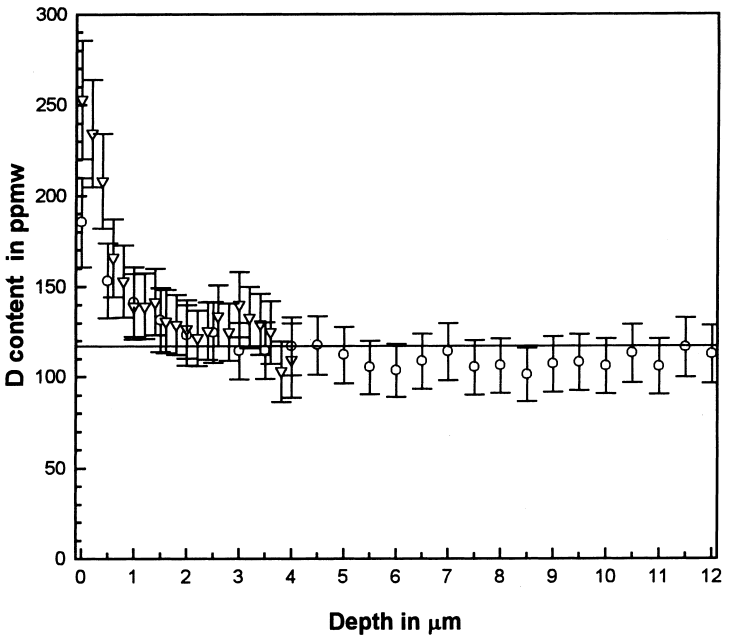

Fig. 3. Concentration of D as a function of depth extracted from the NRA measurements: 2 MeV (▽) and 4.5 MeV (○). The solid line shows the HVEMS result of 117 ppmw.

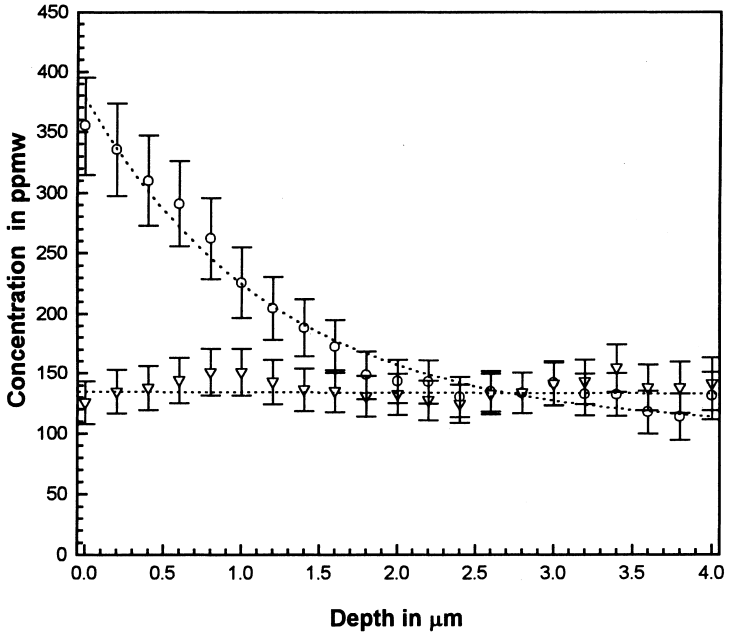

Fig. 4. Concentration of D as a function of depth measured immediately after cutting (○) and after a careful polishing cycle (▽). The dotted lines are for guiding the eye only.

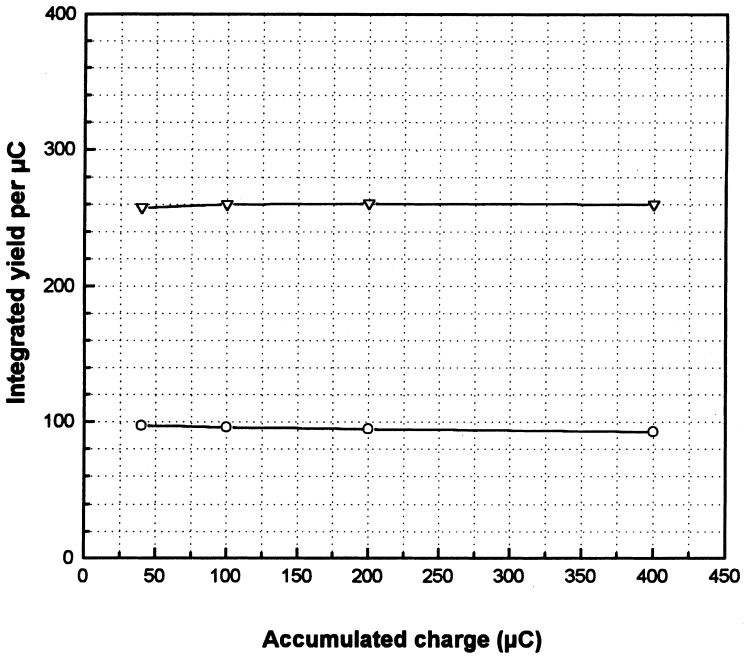

Fig. 5. Fluence dependence of the integrated proton yield measured for 2 MeV incident ^{3}He ions. The data are shown for different depth regions by choosing appropriate windows (see abscissa depth scale at top in the spectrum shown in Fig. 2(a)): 0–1.5 μm (○) and 1.5–3.9 μm (▽).

The surface enhancement is observed from samples immediately after cutting by a low speed diamond saw, indicating that the defects and stress generated during cutting attract D atoms to the damaged region which

extends to a depth of ~1 μm. Such enhancement can be reduced or even eliminated by a careful polishing. Fig. 4 shows that the surface enhancement was observed on a freshly cut sample, but disappeared after several polishing cycles with 600 grit sanding paper. The effects of cutting and polishing on the distribution of D are under a separate investigation.

In light of the effects attributed to ion beam fluence that have been observed earlier [4], we have examined the integrated proton yield as a function of accumulated charge using 2 MeV $^3He^+$ ions. The results are shown in Fig. 5. The uncertainties are statistical only and therefore small in this case (<1.6%). For the near-surface region (depths $\leqslant$ 1.5 μm), a slight loss of D with increasing ion beam fluence is apparent (the lower curve). However, for greater depths corresponding to the region characterized by a 'bulk' concentration, no loss of D is observed for incident fluences up to 400 μC. We should point out that the fluences used earlier [4] started from ~100 μC and exceeded those used here by approximately a factor of 5. It is obvious from Fig. 5 that D depth distributions can be obtained using modest ^{3}He ion fluences, e.g. ~50 μC, at a current density ~0.025 A m^{-2}.

4. Conclusions

In contrast to conclusions reached in an earlier study [4], we have found that ion beam desorption effects can be safely circumvented with regard to measurement of bulk deuterium concentration values. The D depth profile in a sample can be precisely and non-destructively determined by deconvolution of the corresponding proton energy spectrum, incorporating the effects of energy loss straggling, multiple scattering, finite detector size, finite beam spot size, etc. Analyses using beams at energies of 2 MeV and 4.5 MeV are consistent and in good agreement with bulk D concentration values measured by HVEMS.

Acknowledgements

Financial support from CANDU Owner's Group (WPIR #3517) is gratefully acknowledged. The authors wish to thank Dr S.J. Bushby of AECL for help in analysing the samples by HVEMS.

References

[1] D.O. Northwood, U. Kosasih, Int. Met. Rev. 28 (1983) 92.
[2] T. Schober, H. Wenzl, in: G. Alefeld, J. Völkl (Eds.), Hydrogen in Metals, Springer, Berlin, 1978.
[3] J. R. Tesmer, M. Nastasi (Eds.), Handbook of Modern Ion Beam Materials Analysis, Materials Research Society, Pittsburgh, PA, 1995.
[4] T. Laursen, R. Koelbl, J. Nucl. Mater. 137 (1986) 241.
[5] W.N. Lennard, G.R. Massoumi, P.F.A. Alkemade, I.V. Mitchell, Nucl. Instr. and Meth. B 73 (1993) 203.
[6] W. Möller, F. Besenbacher, Nucl. Instr. and Meth. 168 (1980) 111.
[7] J.L. Yarnell, R.H. Lovberg, W.R. Stratton, Phys. Rev. 90 (1953) 292.
[8] D. Dieumegard, D. Dubreuil, G. Amsel, Nucl. Instr. and Meth. 166 (1979) 431.
[9] W.N. Lennard, H. Geissel, K.B. Winterbon, D. Phillips, T.K. Alexander, J.S. Forster, Nucl. Instr. and Meth. A 248 (1986) 454.
[10] W.N. Lennard, H. Geissel, D. Phillips, R. Hill, D.P. Jackson, Nucl. Instr. and Meth. B 10&11 (1985) 592.
[11] J.F. Ziegler, Helium: Stopping Powers and Ranges in All Elements, Pergamon, New York, 1977.